TRANSIENT 3-D NEUTRON KINETIC ANALYSIS WITH CORETRAN OF A CORE THERMAL-HYDRAULIC BOUNDARY CONDITION MODEL PEACH BOTTOM 2 TURBINE TRIP BENCHMARK PHASE 2

Hakim Ferroukhi and Werner Barten
Paul Scherrer Institut
CH-5232 Villigen PSI, Switzerland
Hakim.Ferroukhi@psi.ch , Werner.Barten@psi.ch

Paul Coddington
Paul Scherrer Institut
CH-5232 Villigen PSI, Switzerland
Paul.Coddington@psi,ch

ABSTRACT

This paper presents the results of the OECD/NRC BWR Peach Bottom 2 (PB2) turbine trip (TT) benchmark Exercise 2a obtained at the Paul Scherrer Institute (PSI) using the CORETRAN code. This CORETRAN analysis of exercise 2a, in which, a 3-D core kinetic model with pre-defined transient core boundary thermal-hydraulic conditions is used to simulate the PB2 TT test 2 (TT2), represents the first attempt at PSI to assess the code for a transient case where the core behavior is a response to a Thermal-Hydraulically related perturbation. To start, a description of the CORETRAN model and how the different specifications were taken into account for the PB2 analysis is given in order to illustrate that it is truly the nominal CORETRAN results, i.e. when strictly following the benchmark specifications, that are here presented. Thereafter, the steady-state results, based on a detailed BWR flow split model, are presented at the initial conditions of TT2 as well as for a hypothetical Hot-Zero-Power (HZP) case. For the TT2 case, the results show a good agreement with data measured by the online process computer of PB2 prior to the test. The transient analysis is thereafter performed using as boundary condition, time-dependant functions of the core exit pressure, the core inlet subcooling and individual channel mass flows, all provided as part of the specifications. The calculated fission power is found to be very close to the measured one when using this boundary condition model. In addition, the change in global and local power distribution predicted by CORETRAN during the unscrammed phase of the transient is discussed.

1. INTRODUCTION

At PSI, the CORETRAN code [1] is used for the 3-D kinetic analysis of transients where only the core dynamical behavior is of interest. The reason is that the code is principally built on a coupling between the ARROTTA 3-D neutronic code with the VIPRE-02 Thermal-Hydraulic (T/H) code and aimed at performing steady-state and transient analyses of full core inlet-to-outlet models. A continuous effort to verify the capabilities of CORETRAN for different types of 3-D core analyses is currently being performed at PSI. So far, the assessment of the code has only been carried-out for steady-state applications [2] and for neutronically-driven transients such as Reactivity-Initiated-Accidents [3].

Although both these types of applications have provided confidence in the 3-D core analysis capabilities of the code, it was nevertheless considered appropriate to also assess the code for T/H driven transients. In that perspective, the TT benchmark exercise 2a aimed at predicting the core dynamical response to pre-defined T/H transient boundary conditions appeared as a very well suited test case and has therefore been analyzed. This paper presents the developed CORETRAN PB2 core model and the results obtained with that code for Exercise 2a.

2. MODELLING

2.1. CORETRAN PB2 CORE MODEL

According to the benchmark specification report [4], the PB2 core comprises 764 fuel assemblies, each one belonging to one of two fuel types included in the cycle 2 (7x7 and 8x8), 185 control rods and 43 LPRM strings. Since CORETRAN is intended for full core analyses, the radial assembly representation shown in Figure 1 is selected to model the cycle 2 core.

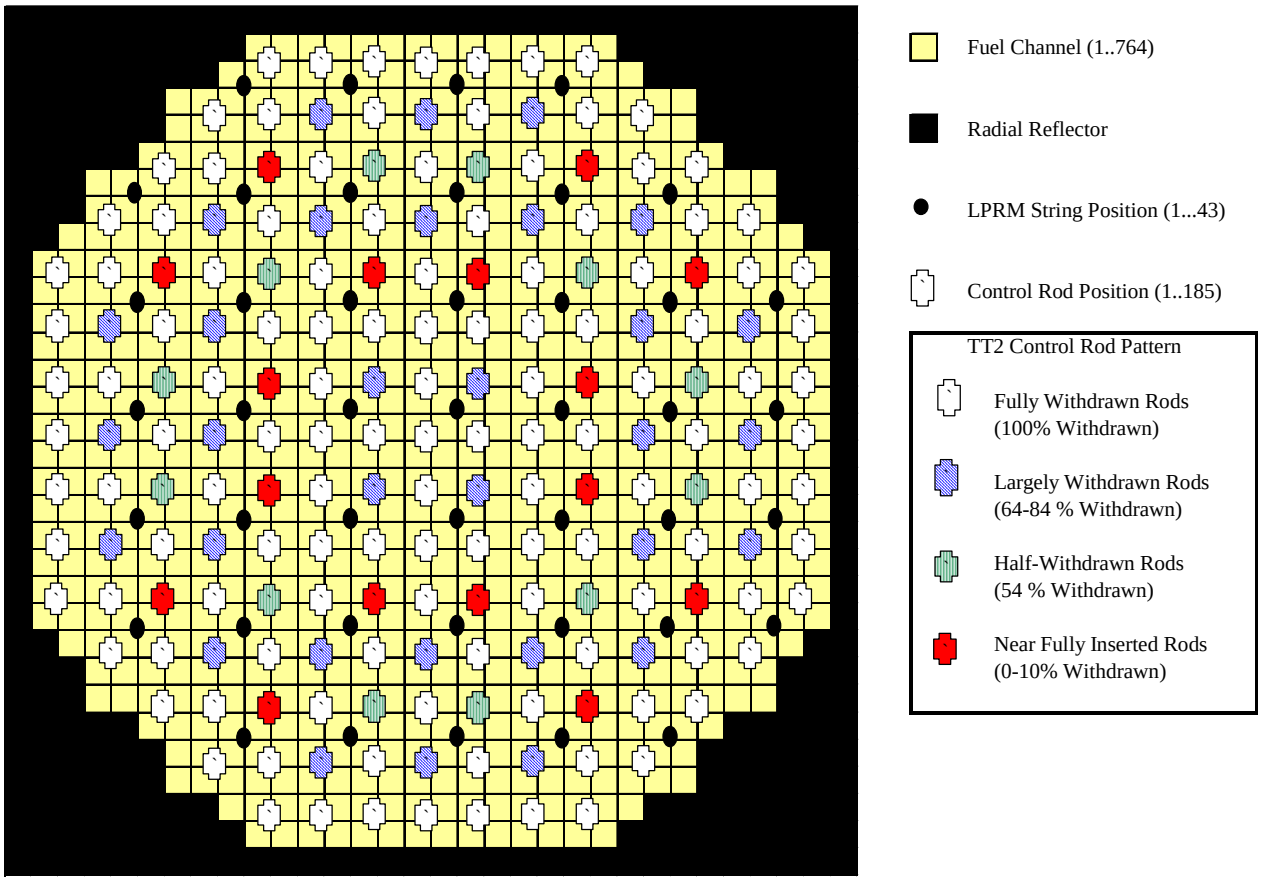

Figure 1. CORETRAN Radial Representation of the PB2 Core

As mentioned previously, CORETRAN is truly a coupling between the ARROTTA neutronic module and the VIPRE-02 Thermal-Hydraulic (T/H) module. The neutronic modeling is hence implemented via the ARROTTA module where each fuel assembly (including the radial reflectors) is represented as a neutronic channel divided into 26 axial nodes (with both the height and the radial pitch set to

15.24 cm), and where the control rod as well as the LPRM strings positions (radial and axial) are specified.

The T/H model is implemented via the VIPRE-02 module and consists also of 764 individual separated channels where 1-D coolant flow is assumed. In addition, the T/H model includes an additional channel to represent the core bypass region. With regard to the axial representation of the T/H channels as well as the coupling to ARROTTA, it is important to emphasize that CORETRAN is truly a core-only analysis code. For that reason, the modeling shown in Figure 2 is used.

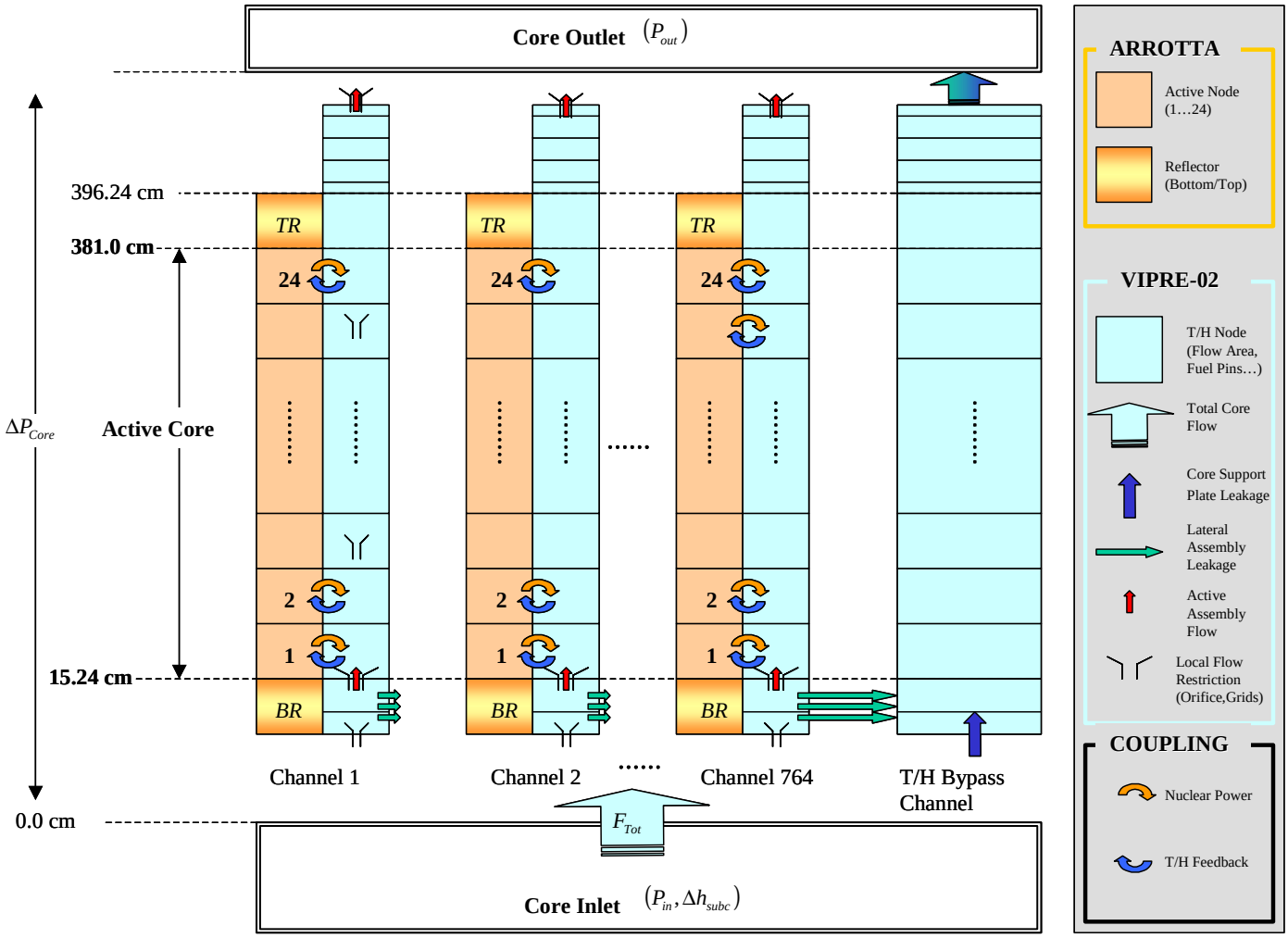

Figure 2. CORETRAN PB2 Axial Core Representation – ARROTTA/VIPRE-02 Coupling

As shown in Figure 2, the T/H modeling is made from the core inlet to the core outlet with an axial nodalization of the T/H channels selected so that in the active core region, it corresponds exactly to the ARROTTA nodalization while the channel inlet region below the active part is divided into two nodes to model the complex mechanical structure of the inlet region of BWR fuel assemblies. Similarly, the channel region above the active part is extended and split into 5 axial nodes in order to correctly define the mechanical structure of the BWR fuel assembly exit region. With this T/H nodalization, the mechanical design data specified in [4] (flow area, hydraulic diameter, wetter perimeters, fuel pins geometry, fuel heat transfer data, pressure loss coefficients) are thereafter assigned to each of the 765 T/H channels (i.e. including the bypass).

2.2 BOUNDARY CONDITIONS AND CALCULATIONAL OPTIONS

The objective of exercise 2a is to perform the three following calculations using pre-defined core T/H boundary condition:

1. Steady-State Calculation at the TT2 initial conditions

2. Steady-State Calculation for a hypothetical HZP case

3. Transient Calculation of the TT2 test

To perform all these calculations, the CORETRAN PB2 model (see previous section) along with the calculational options described here is used.

Neutronic Options

For the neutronic calculations, there exists in CORETRAN two 3-D 2-group diffusion algorithms. Both are based on the Analytical Nodalization Method (ANM) but differ in that the solution scheme in the first algorithm uses an iterative matrix inversion method [5] while the second algorithm is based on a non-linear CMFD iteration method [6]. In the analyses presented here, the first of these algorithms, referred to as the A-N model, has been used.

Concerning the Cross-Section (X-S) model, the 435 different nuclear data sets included in the specifications for both controlled and uncontrolled nodes are read directly by the code while the multi-dimensional X-S interpolation routine, also provided as part of the specifications, is implemented in the code. This is done in order to strictly follow the specifications but implies that the nominal CORETRAN X-S model is hence not used here. Moreover, a X-S correction upon the Xenon distribution at the TT2 initial conditions is according to the specifications implemented for the TT2 cases (steady-state and transient) while this correction is not performed for the HZP static case.

Another modification that is implemented with regard to the X-S model, and which is thus not standard in the code, is the correction of the effective nodal moderator density in a given active node upon the bypass coolant properties weighted by the local bypass to active flow area ratio:

$$\rho_{eff} = \rho_{act} + \left[\frac{A_{byp}}{A_{act}} \cdot \left(\rho_{byp} - \rho_{byp,SAT} \right) \right] \qquad (1)$$

Note that when implementing this correction in CORETRAN, the same area ratio (Eq. 1) is assigned to all active nodes, based on the approximation that the local bypass area and the active node flow area remains fairly constant over the whole core.

Finally, the CORETRAN code does at the moment not include a decay heat model and such model is hence not used in the results presented in this paper.

Thermal-Hydraulic Options

For all T/H calculations, the VIPPRE-02 two-fluid 6-equations algorithm is used. Concerning the flow split model to calculate the BWR active flow as well as the total bypass flow, the most advanced option in the VIPRE-02 module is based on the FIBWR algorithm [7] with the total core flow (F_{Tot}) and the core exit pressure (P_{out}) as boundary conditions. This algorithm performs a flow split calculation, taking into account different types of leakage to represent the bypass flow, in order to obtain a uniform core pressure drop (ΔP_{Core}) over all T/H channels. To calculate the bypass flow (and hence the individual channel active flows), the FIBWR procedure is based on representing each leakage flow defined in the model, by means of a correlation expressing the leakage flow from node *x* to node *y*, $W_{x\to y}$, as function of the pressure differential ΔP_{x-y} weighted to the local density (ρ) properties.

$$W_{x\to y} = \left(K_1 \cdot \Delta P_{x-y}^{1/2} + K_2 \cdot \Delta P_{x-y}^{K_4} + K_3 \cdot \Delta P_{x-y}\right)\sqrt{\frac{\rho_x}{\rho_{ref}}} \qquad (2)$$

For the PB2 model, the following leakage flows are modeled: three lateral leakage paths out of the inlet part of the fuel assemblies and the leakage through the core support plate (see Figure 2). Note here that one of the modeled lateral leakage path is used, similarly as has been done for the Swiss BWR CORETRAN models [2], to simulate the intra-assembly water paths (i.e. water rods).

For each leakage path, the coefficients $K_i\left(i = 1\cdots 4\right)$ of Eq. 2 are entered as input in the VIPRE-02 input model. Concerning the PB2 model, they were selected as follow, recalling that these were not defined in the benchmark specifications. For the assembly specific leakage flows (i.e. lateral leakage and water rods), data used in the PSI CORETRAN models of Swiss BWRs were assigned to the PB2 model taking into consideration the type of fuel (7x7 and 8x8) inserted in the core. Nominal data (i.e. unmodified from the correlations used in the PSI models) were implemented. Concerning the core support plate leakage, the correlation used for a Swiss large BWR model was assigned to the PB2 model.

Now, it must be emphasized that the FIBWR algorithm is of steady-state nature. Therefore, while it represents the most detailed code option for steady-state flow split calculations and is consequently used for the static calculations presented in this paper (TT2 initial conditions and HZP), it is on the other hand not applicable for transient analyses. This implies that the time-dependant total core flow boundary condition cannot be used since the code does not have an applicable transient flow split procedure. Instead, the pre-defined transient flow split included in the specifications as an alternative to the total core flow boundary condition and where the time-dependant coolant flows in 34 groups of individual T/H channels are provided, is instead used as boundary condition for the CORETRAN transient analysis. It must be here emphasized that the 34-group T/H transient flow functions are, prior to performing the analysis, decomposed and specified in CORETRAN as individual transient active flows for all 764 T/H channels and for one bypass channel. This is done since the main objective is to perform a full core neutronic-T/H coupled analysis.

It must also be emphasized that there exists at the moment no possibility in CORETRAN to take into account bypass heating due to the nature of the coupling between ARROTTA and VIPRE-02 where only the active core nodes (i.e. exclusive bypass and reflectors) are “connected”.

A summary of the CORETRAN calculational options for the PB2 analysis is given in Table 1.

CALCULATIONAL OPTION		**STEAD-STATE**	**TRANSIENT**
NEUTRONIC MODEL	Algorithm	A-N	A-N
	X-S Model	Specified [4]	Specified [4]
	Bypass Density Correction	Yes	Yes
	Thermal X-S Xenon Correction	• Yes (TT2) • No (HZP)	Yes
	Decay Heat	*Not Used*	*Not Used*
T/H MODEL	Algorithm	2-Fluid 6 Equations	2-Fluid 6 Equations
	Boundary Conditions and Flow Split	FIBWR Algorithm with • Core Exit Pressure • Core Uniform Inlet Subcooling • Core Total Inlet Flow	Transient Functions of • Core Exit Pressure • Core Uniform Inlet Subcooling • Individual Active Flow for all 764 T/H Channel + Bypass Flow
	Direct Moderator Heating	2%	2%
	Bypass Heating	*Not Available*	*Not Available*
	Water Steam Properties	Evaluated at Core Exit Pressure	Evaluated at Core Exit Pressure

Table 1. CORETRAN Calculational Options for PB2 Analysis

2.3 OPERATING CONDITIONS

The operating conditions for the steady-state and transient analysis of the TT2 case used in the CORETRAN calculations are shown in Table 2. The hypothetical HZP conditions are also shown in the same table. Moreover, the data used in the CORETRAN transient analysis are also given.

ANALYSIS INPUT DATA		**TT2**	**HZP**
Steady-State	Reactor Power	2030 MW	32.93 MW
	Total Core Flow	10445 kg/s	10445 kg/s
	Core Exit Pressure	67.98 bar	67.98 bar
	Core Inlet Subcooling	48005.3 J/kg	• Fuel Temperature = 552.833 K • Coolant Density = 753.977 kg/m3
Transient	Time-Step Size	0.001 s	*No Transient Analysis*
	SCRAM Data	SCRAM Starts at t=0.75s	
	Rod Speed During SCRAM	Constant Speed: • V=0.713 m/s for $0.75 \leq t < 0.79$ s • V=1.423 m/s for $t \geq 0.79$ s	

Table 2. Operating Conditions and Transient Data for CORETRAN Analyses

3. STEADY-STATE RESULTS

A summary of the CORETRAN steady-state results for Exercise 2a is given in this section. To start, the core average normalized axial power distribution and the core average axial void fraction calculated by CORETRAN at the TT2 initial conditions is shown in Figure 3. In the same figure, the normalized axial power measured by the PB2 on-line process computer prior to the test and provided in [4], is also presented. This figure shows a good agreement in axial power profile between CORETRAN and the measured data although the CORETRAN axial power factors are slightly larger in the top part of the core while the opposite is observed in the bottom core region. It is at this point difficult to explain these small differences particularly since the "measured" void fraction is not available.

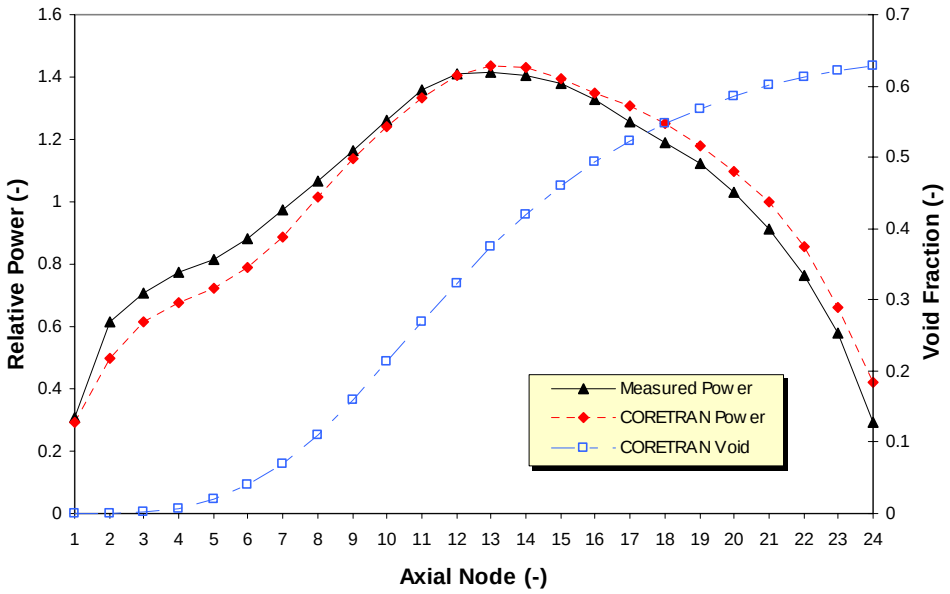

Figure 3. Steady-State Core Average Axial Distributions at the TT2 Initial Conditions

However, when some of the CORETRAN calculated T/H parameters are compared in Table 3 with the available measured data and some data provided in [4], the agreement is found to be quite satisfactory. Clearly, the Table 3 results with regards to the core pressure drop and the bypass flow fraction indicate, that the FIBWR algorithm based on leakage correlations "borrowed" from the Swiss BWR models performs in a satisfactory manner and predicts adequately this two T/H parameters. It is also noted that the core exit quality calculated by CORETRAN is identical to the one recalculated from the measured data [4] while the average void fraction is slightly larger.

Finally, a summary of the static neutronic results is given in Table 4 for both the TT2 and the HZP cases. In that table, the effective multiplication factor (K_{eff},) the core average axial peaking factor as well as the maximum nodal power factors for the assemblies 75 and 367 (F_z), the core average maximum radial peaking factors (F_{rad}) and the core maximal nodal peaking factor (*npf*) are specified. In Table 4, it is seen that the predicted K-eff is very large at the initial TT2 conditions while as expected because of the operating conditions (checkerboard control rod pattern at low power and Xenon nodal densities from nominal operation), a much lower value is obtained for the HZP case.

CORE T/H CORE-PARAMETER		**CORETRAN**	**CALCULATED (SPECIFIED IN [4])**	**MEASURED (PROVIDED IN [4]**
Pressure Drop (bar)		1.063	1.136	0.836
Exit Quality (%)		0.097	---	0.097*
Void Fraction (-)		0.319	---	0.304*
Bypass Flow (%)	Total	8.61	8.06	---
	Lateral Leakage + Water Rods	5.84	5.48	---
	Core Support Plate Leakage	2.77	2.58	---

*) Recalculated from PB2 On-Line Process Computer

Table 3. Comparison of CORETRAN T/H Static Results with Specified and Measured Data at TT2 Initial Conditions

The large K-eff value for the TT2 case is difficult to explain particularly since as shown by Table 3, the core average void fraction appears to be larger than the measured one. Combining this observation with the larger axial power in the upper part of the core predicted by CORETRAN (Fig. 3), a possible explanation would be that the void-coefficient, implicitly obtained via the provided cross-sections, is underpredicted in CORETRAN.

CORE NEUTRONIC PARAMETERS		**TT2**	**HZP**
K_{eff}		1.00713	0.99719
F_z^{node}	Core Average	1.4339^{13}	2.7157^{21}
	Channel 75	1.0042^{12}	2.1443^{20}
	Channel 367	1.7275^{13}	3.3238^{21}
$F_{rad}^{Channel}$		1.466^{395}	2.0021^{457}
$npf_{rad}^{Channel.node}$		$2.1843^{468,13}$	$5.4210^{457,21}$

Table 4. Summary of CORETRAN Static Neutronic Results

Finally, the core average radial power distributions obtained for both the TT2 initial conditions and the HZP case is shown in Figure 4.

TT2 Radial Power HZP Radial Power													
								0.37 0.13	0.52 0.22	0.58 0.40	0.62 0.43	0.64 0.29	0.65 0.30
						0.45 0.26	0.73 0.35	0.95 0.49	0.96 0.71	1.09 0.81	1.04 0.57	1.14 0.62
				0.31 0.17	0.49 0.22	0.73 0.38	1.00 0.81	0.97 0.82	1.14 0.71	1.06 0.69	1.29 1.10	1.14 0.97
				0.53 0.34	0.80 0.43	1.00 0.62	0.90 0.87	0.96 0.94	1.01 0.76	1.07 0.78	1.13 1.05	1.15 1.04
			0.47 0.21	0.77 0.42	1.04 0.90	0.91 0.91	0.78 0.82	0.73 0.81	1.18 1.32	1.10 1.15	1.22 0.95	1.08 0.87
		0.31 0.17	0.53 0.34	0.78 0.42	1.06 0.64	0.98 0.92	0.98 1.04	0.73 0.84	0.75 0.89	1.04 1.21	1.11 1.22	1.06 0.93	1.07 0.93
		0.49 0.22	0.80 0.44	1.04 0.91	0.98 0.92	1.15 0.85	1.02 0.85	1.17 1.40	1.03 1.24	1.22 1.06	1.09 0.98	1.27 1.52	1.10 1.30
	0.45 0.26	0.72 0.39	1.00 0.63	0.91 0.92	0.98 1.05	1.01 0.85	1.05 0.91	1.07 1.25	1.09 1.27	1.09 1.01	1.07 1.03	1.05 1.37	1.04 1.38
0.37 0.14	0.73 0.35	1.00 0.82	0.89 0.88	0.78 0.84	0.73 0.85	1.17 1.42	1.07 1.26	1.18 1.08	1.05 1.02	1.29 1.61	1.07 1.41	0.88 1.19	0.79 1.10
0.51 0.23	0.94 0.50	0.97 0.84	0.97 0.98	0.73 0.83	0.76 0.91	1.03 1.27	1.09 1.30	1.05 1.03	1.07 1.06	1.13 1.42	1.09 1.43	0.82 1.11	0.81 1.12
0.57 0.41	0.95 0.72	1.14 0.73	1.00 0.78	1.17 1.35	1.04 1.23	1.22 1.08	1.09 1.03	1.29 1.65	1.14 1.46	1.34 1.22	1.14 1.12	1.27 1.75	1.09 1.49
0.61 0.44	1.09 0.84	1.07 0.72	1.06 0.81	1.10 1.18	1.11 1.26	1.09 1.00	1.08 1.06	1.08 1.45	1.10 1.49	1.15 1.13	1.19 1.15	1.18 1.52	1.18 1.52
0.63 0.30	1.06 0.60	1.29 1.15	1.13 1.09	1.22 0.99	1.06 0.97	1.28 1.58	1.06 1.41	0.89 1.22	0.82 1.14	1.28 1.78	1.18 1.54	1.34 1.30	1.18 1.20
0.65 0.31	1.15 0.64	1.15 1.01	1.15 1.09	1.08 0.91	1.07 0.97	1.10 1.35	1.04 1.41	0.79 1.12	0.81 1.15	1.09 1.52	1.19 1.54	1.18 1.21	1.22 1.22

Figure 4. CORETRAN Steady-State Relative Radial Power Distributions

4. TRANSIENT RESULTS

3.1 REACTOR FISSION POWER

The transient calculation of the TT2 Exercise 2a is performed according to Table 1 recalling mainly that the FIBWR flow split model is not used but instead, the time-dependant flow in all 765 T/H channels (i.e. including in the bypass channel) is specified as boundary condition. The calculated fission power, normalized to the initial core fission power, is shown in Figure 5 along with the normalized measured fission power provided from the benchmark specifications for Exercise 1 ([4]). The CORETRAN transient reactivity components are also shown in the same figure.

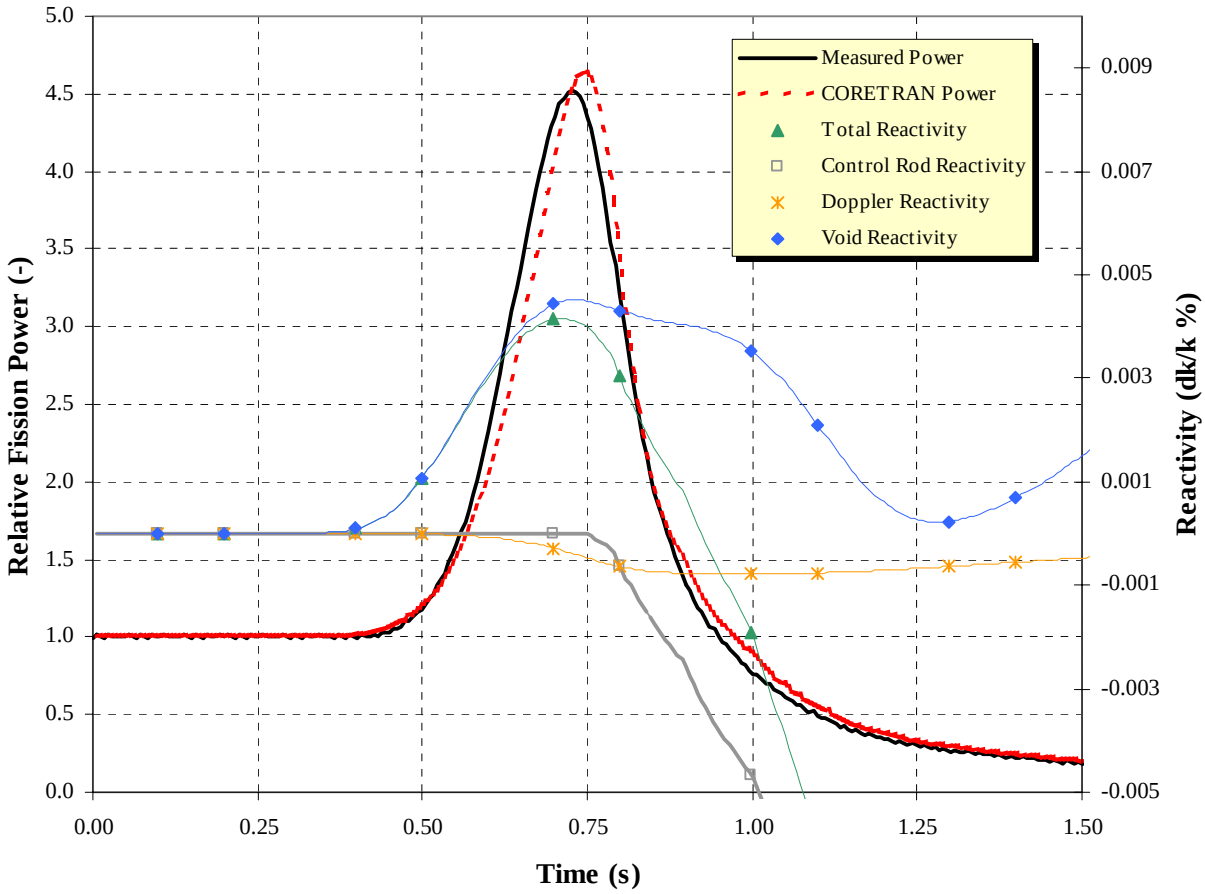

Figure 5. CORETRAN Reactor Fission Power and Reactivity Components

Although not seen clearly in Fig.5, the maximum fission power predicted by CORETRAN occurs at t=0.741 s i.e. just before the instant when SCRAM is activated (t=0.75s), indicating that the power is according to CORETRAN reversed by the decrease in void reactivity combined with the increased negative Doppler feedback. The Doppler increases because of the heat generated during the power increase phase. Concerning the positive void reactivity, it starts being reduced at around 0.70 s due to two effects: the first is that the rate of the core exit pressure increase (due to the pressure wave) is reduced at around 0.70 s, recalling that this is a boundary condition to the calculation. This means that at around that time, the void collapsing is "slowed down". The second effect is that the large reactor power increase implies that void starts being produced by Direct Moderator Heating (DMH) while at the same time, heat conducted from the fuel pellets to the coolant also contributes to the void production. Because these two phenomena produce void, they thus have a counterbalancing effect to the void collapsing resulting from to the pressure wave. If the CORETRAN reactivity results are considered, it appears hence that the void production rate (i.e. from DMH and from fuel heat conduction) becomes larger than the void collapsing rate and the void reactivity consequently starts being reduced. Combined with the increase of the negative Doppler feedback, the total reactivity starts to decrease and the fission power is therefore reversed since the core never reaches prompt criticality. The above discussed CORETRAN result is consistent with what was observed during the test since as seen in Figure 5, the measured fission power was reversed before SCRAM was activated indicating that the power excursion was indeed terminated by the T/H feedback (negative Doppler reactivity and decrease of the void reactivity).

It is also interesting to notice that the CORETRAN power peak magnitude is in very good agreement with the measured value although slightly larger. Moreover, a steeper power decrease phase is noticed in CORETRAN but this is due to the smaller delay (between the power reversal and the SCRAM activation) predicted by the code compared to the measurement. Indeed, in the measured data, a slightly larger time is elapsed between the instant when the power reaches its maximum and the moment at which SCRAM is activated. During that time, the power reversal is guided by the core negative reactivity increase due to the T/H feedback and the rate at which this occurs is smaller than the negative reactivity-insertion rate induced by a SCRAM. Also, it must be emphasized that the control rod speed used in CORETRAN (Table 2) was based on average rod motion values specified in [4]. Since it is highly probable that these average values were slightly different from the actual speed at which the rods were truly inserted during the test, small deviations in the rate of the power decrease after SCRAM can be expected between the calculation and the measurement.

3.1. LPRM DETECTOR RESPONSES

In order to investigate the CORETRAN predictions of the local changes in neutron fluxes occurring during the transient, the calculated LPRM detector responses are studied. In the PB2 core, there are 43 LPRM strings and each one contains 4 detector chambers located at the axial core heights 45.72 cm (A), 137.16 cm (B), 228.6 cm (C) and 320.04 cm (D) respectively. In Figure 6a, the absolute signals in each of the 4 axial locations averaged over all 43 strings are shown.

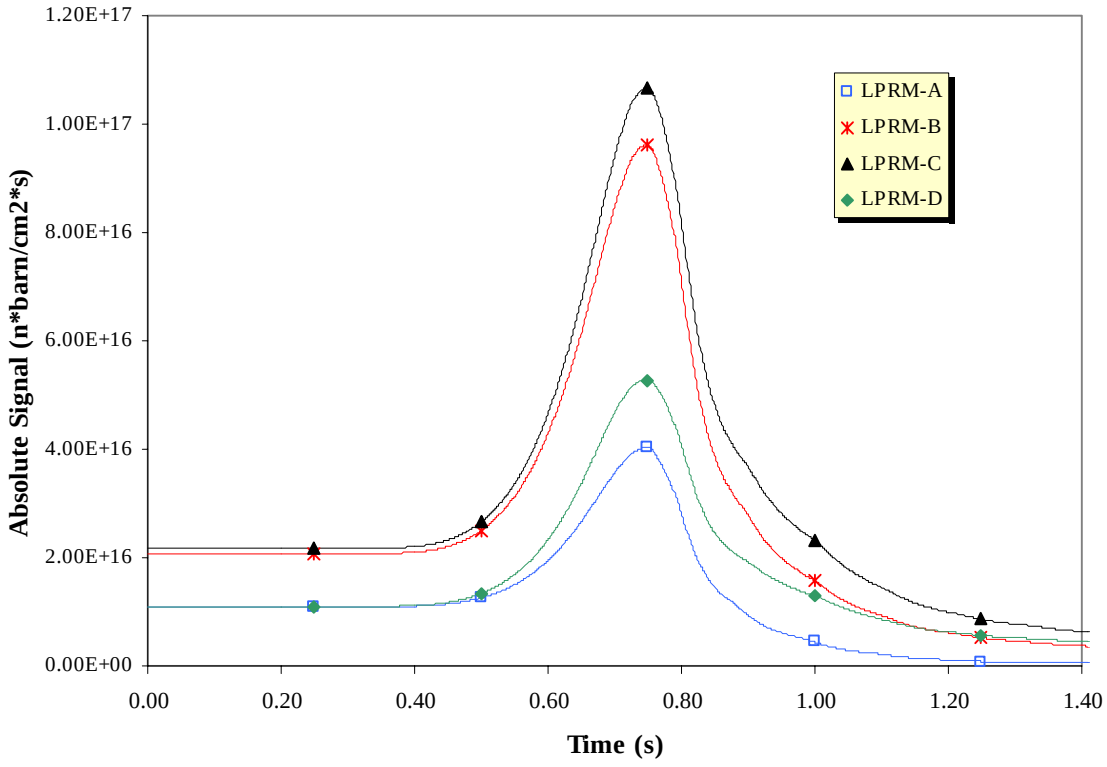

Figure 6a. CORETRAN Calculated Core Averaged LPRM Signals (Absolute)

From Figure 6a, it is seen that the detector signals, which illustrate the neutron flux at 4 distinct axial positions in the core, are largest for the LPRM-C signals followed by the LPRM-B signals whereas the signals in LPRM-A and LPRM-D are significantly smaller. If the steady-state axial power distribution is considered, (Figure 3) it can be seen that this ranking of the detector signals with regard to their magnitude is consistent with the ranking of the initial peaking factors for these 4 axial locations (noting that detector A is located between nodes 3 and 4, detector B between nodes 9 and 10, detector C between nodes 15 and 16 and detector D between nodes 22 and 23). The LPRM signals up to SCRAM are hence consistent with the initial steady-state axial power distribution indicating that during the small elapsed time up to SCRAM, and also after SCRAM is activated, the core averaged normalized axial power distribution is not significantly changed i.e. the normalized axial power shape remains similar to the initial power profile. In turn, this illustrates the importance of predicting adequately the initial steady-state power profile for this type of analysis.

Figure 6b below shows the same LPRM signals normalized to their initial value signals to illustrate here the relative change in neutron flux as function of core axial position.

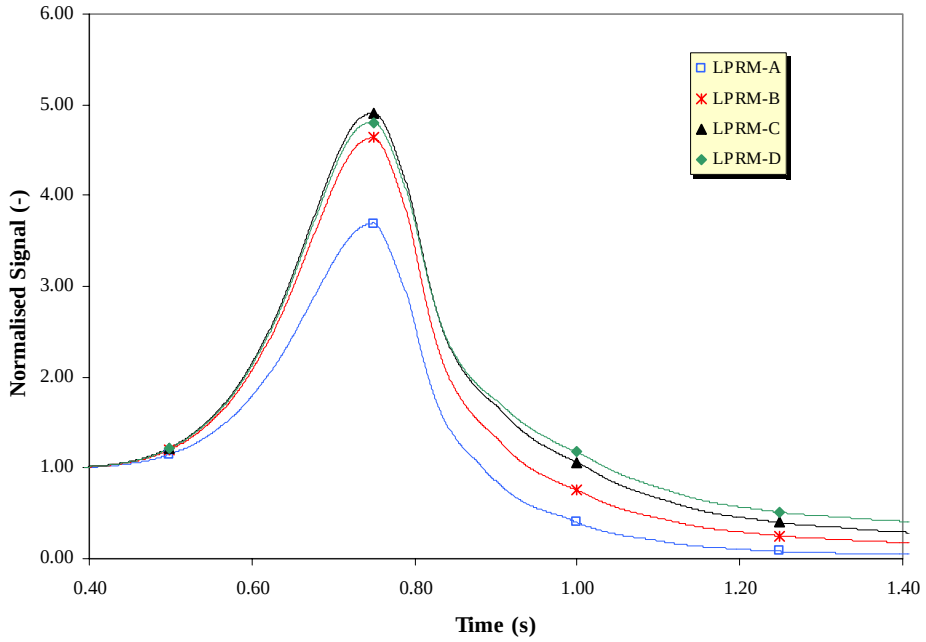

Figure 6b. CORETRAN Calculated Core Averaged LPRM Signals (Normalized)

The figure above shows that during the power excursion and before SCRAM is activated, the relative increase in the average detector response is largest for LPRM-C followed by LPRM-D, LPRM-B and finally LPRM-A, indicating that for all these 4 axial positions, the largest increase in fission power and neutron fluxes is obtained in the middle and upper core regions i.e. in the highly voided core zones. This is because the void coefficient is there larger compared to the lower core regions and therefore, the void collapsing effect on the local power increase will hence be much stronger. The strongest local power increase is obtained for axial core regions where the (thermal) flux magnitude is large in combination with a highly negative local void coefficient. For example, the strongest relative power increase is seen in Figure 6b for LPRM-C, which is located in a core region with a relatively large void content (and thus with a strongly negative local void coefficient) and characterised by the highest local flux magnitude (see Figure 6a). On the other hand, even though the LPRM-B is characterised by a higher local flux magnitude compared to LPRM-D, the relative power increase is

larger in LPRM-D because of the stronger local void coefficient. Note that these results are however also affected by the fact that the calculation is performed with the water steam properties evaluated at the core exit pressure. Hence, the pressure wave propagation down the core is not taken into account. It is however assumed that this should have a rather small impact on the results discussed here i.e. the same trend as seen in Figure 6a and 6b should be obtained even with local water properties evaluation but this remains to be further investigated.

3.2. RADIAL POWER DISTRIBUTION

The previous section discussed, by illustrating the LPRM detector responses, how the neutron fluxes were affected during the transient as function of the axial core position. In a similar manner, the change in the 2-D radial power distribution during the transient is here discussed. In the upper part of Figure 7 below, the relative 2-D radial power distribution at the start of the transient is shown while the lower part shows the distribution at the time of the power maximum.

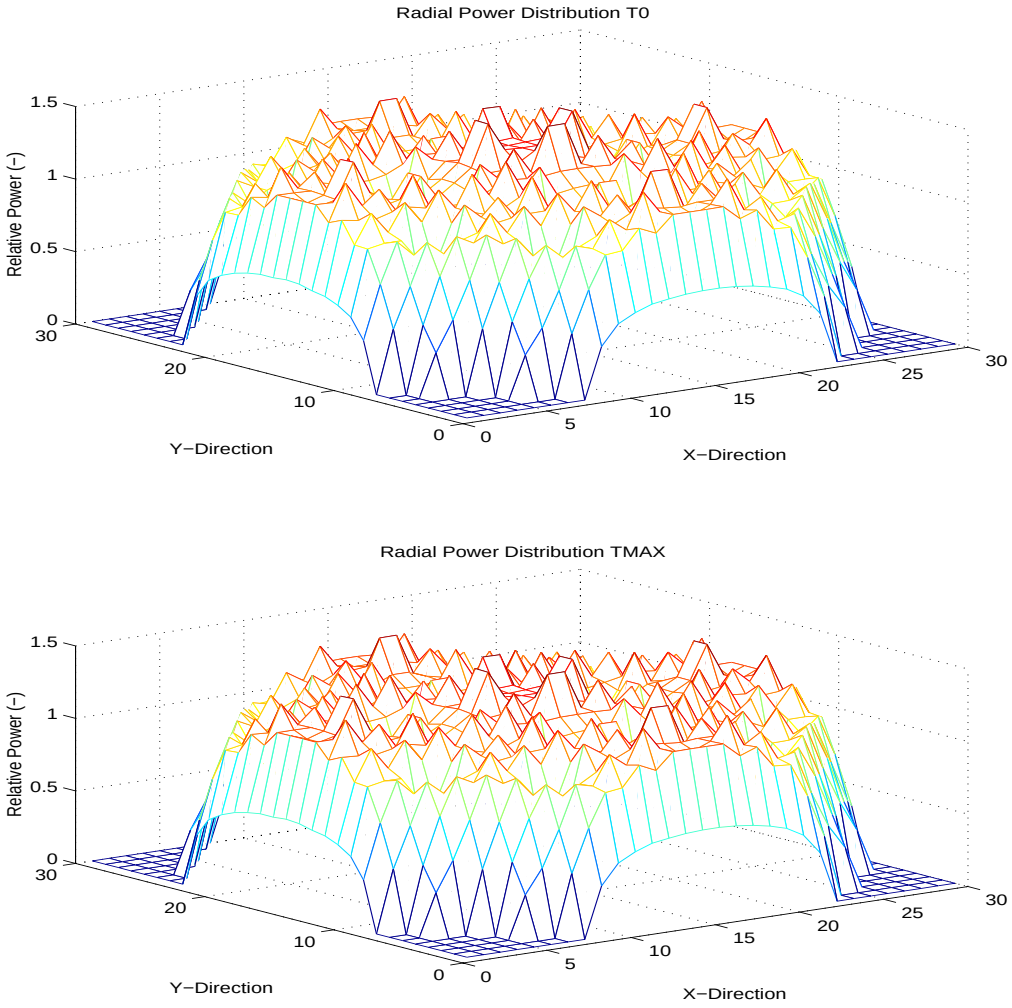

Figure 7. CORETRAN Radial Power Distribution

The results of Figure 7 show that the radial power distribution does not change significantly from a qualitative point of view during the power excursion phase of the transient (i.e. up to the power maximum). However, to investigate the changes on a quantitative basis, the relative change in power distribution during that time is shown in Figure 8. In that figure, orange to red regions represent areas where the radial peaking factors have increased while lighter colored positions (i.e. green, yellow and blue) represent zones where the radial factors are decreased (note that the black color is assigned to non-fuel positions outside the core).

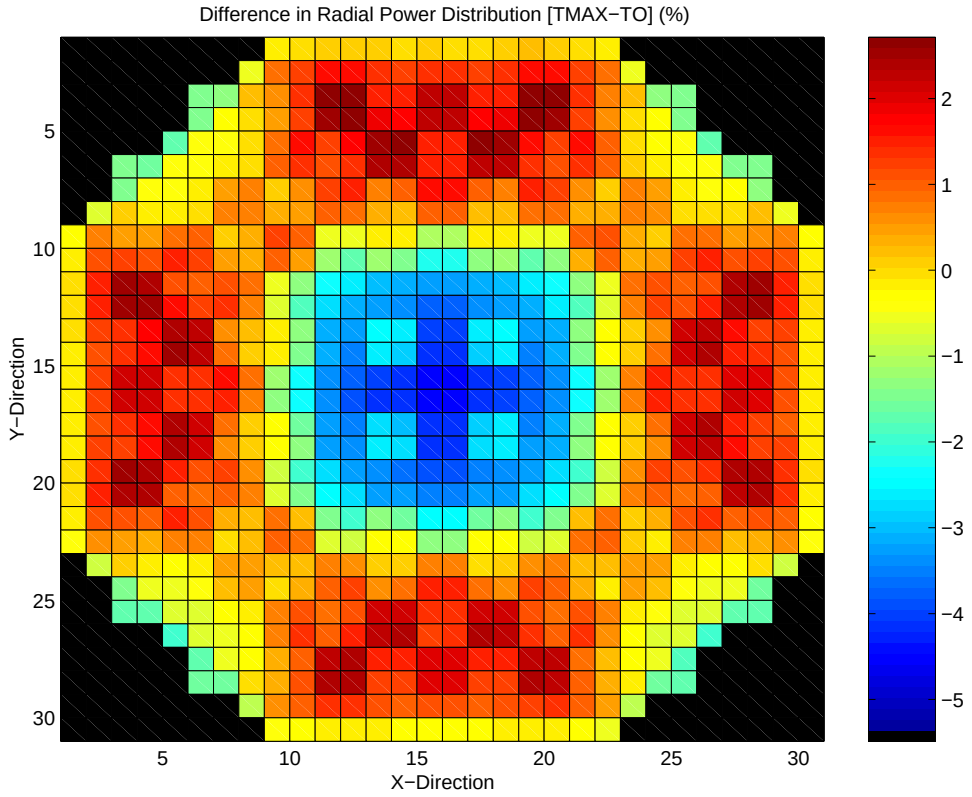

Figure 8. 2-D View of the Relative Change in Radial Power between Time of Power Maximum and Initial Conditions

As can clearly be seen in this figure, the central core region is characterized by a decrease in relative radial power. Similarly, in small core regions located in the North-East (N-E), the North-West (N-W), the South-East (S-E) and the South-West (S-W), the relative power is also decreased but to a smaller extent. On the other hand, in the main center-peripheral core region, i.e. the North, West, South and East core regions, the relative power is increased during the transient. If Figure 8 is compared to Figure 1 where the TT2 initial control rod pattern is shown, it appears that this change in 2-D radial power is strongly coupled to the initial control rod pattern. In particular, the highly inserted control rods seem to create a redistribution of the flux into one region where the radial power is increased ("ring" of center-peripheral assemblies) and into a region where it is decreased ("ring" of center assemblies). The ring of center assemblies is surrounded by highly inserted rods while the N/W/S/E part of the center-peripheral zone is characterized by a low control rod density (moderately to largely withdrawn rods). Hence although the power density increases everywhere in the core during the transient (see LPRM signals of Figure 6a and 6b), the fact that the normalized radial power factors are

reduced in the central region illustrates that the power increase due to the pressurization event has had a lower effect there than in the low-rod density regions, recalling that the radial power distribution is a normalized quantity. Hence even though the observed differences in the radial power distribution are not large, the results of Figure 8 clearly indicate that a redistribution of the flux occurs during the transient and that the use of a 3-D kinetic code appears therefore to be adequate in particular if local spatial effects are to be captured correctly.

A possible physical explanation to the observed flux redistribution could be the following. The transient calculation is performed to simulate a core pressurization induced by a turbine trip with the pressurization assumed to be uniform over the core. The main consequence is that a void collapsing will occur because of the pressure increase. Because the void is decreased, the enhanced moderation will reduce the neutron mean free paths and the thermal diffusion lengths. This implies that among others, the region affected by the absorbing effect around a highly inserted rod, will become increasingly narrow. The effect of the rods will hence become local and this could explain the redistribution of the power with regards to the control rod pattern that appears during the transient. At the same time, the enhanced moderation induces a shift towards lower spectral energies so that an increased number of neutrons become thermalised and therefore, the worth of the control rod is increased. Hence although the affected region becomes increasingly narrow around highly inserted rods, the rod worth becomes at the same time locally stronger. Thus, the rod importance becomes stronger for fuel assemblies near or surrounded by many highly inserted rods while it will be decreased in regions far away from control rods. From that point of view, the decrease in relative peaking factors for the central core region versus the increase in peaking factors in the low rod density regions can be expected.

4.4 SUMMARY OF TRANSIENT RESULTS

Finally, a summary of the CORETRAN transient results is given in Table.4 where the maximum for the reactor fission power and the core-averaged LPRM detector are given. In addition, the 3-D power peaking factors (see definition in Section 3) are also presented.

CORE NEUTRONIC PARAMETERS		**TIME OF POWER MAXIMUM (T=0.741 S)**	**END-OF TRANSIENT (T=5S)**
Fission Power* (Measured*)		4.64 (4.53)	0.015 (0.012)
LPRM-A*		3.70	0.019
LPRM-B*		4.63	0.019
LPRM-C*		4.91	0.020
LPRM-D*		4.81	0.018
F_z^{node}	Core Average	1.5378^{14}	1.5044^{13}
	Channel 75	1.1493^{13}	1.7358^{14}
	Channel 367	1.7888^{13}	1.5340^{12}
$F_{rad}^{Channel}$		1.436^{395}	1.282^{463}
$npf_{rad}^{Channel.node}$		$2.3903^{468,13}$	$2.1167^{468,13}$

* Normalized to Initial Value

Table 5. Summary of CORETRAN Transient Results for PB2 TT Benchmark Exercise 2a

5. SUMMARY AND DISCUSSION

This paper has presented the PSI CORETRAN analysis of the PB2 TT Benchmark Exercise 2a aimed at investigating the 3-D core dynamical response to pre–defined transient core thermal-hydraulic boundary conditions. To start, the CORETRAN modeling of the PB2 core with a full core neutronic as well as thermal-hydraulic representation was presented. Thereafter, the steady-state results both at the initial conditions of the TT2 test as well as at hypothetical HZP conditions were given. For the TT2 case, it was shown that CORETRAN, using a BWR flow split procedure based on the FIBWR algorithm, performed very satisfactorily since a good agreement with the measured core axial power distribution as well as with some core thermal-hydraulic parameters such as the core average void fraction and the exit quality was obtained. The transient analysis was thereafter performed using as boundary condition, the transient inlet flow in all fuel assemblies and in the channel representing the bypass region. The reason to use this specification was that the FIBWR flow split algorithm is currently not applicable for transient calculations and therefore, the total core flow cannot be used as boundary condition. This represents a serious code limitation that can however apparently be overcomed by defining properly the individual transient flow in the core channels. Indeed, with the specified individual channel flows as boundary condition, it was found that CORETRAN performed very well with regard to the predicted core fission transient power. In addition, the transient 3-D power re-distribution effects predicted by CORETRAN during the transients were discussed. It was seen that the core-averaged axial power distribution did not change (i.e. in shape) significantly during the transient but that the transient reactor fission power response would be highly dominated by the local flux increase in the core regions corresponding to large initial axial peaking factors. In addition, the initial control rod pattern was found to induce during the transient (i.e. before SCRAM) a decoupling of the core into well separated regions. This result emphasizes that a 3-D analysis is required to adequately capture the dynamical behavior of the core that occurs during the analyzed transient.

It must be emphasized that the objective of this paper was to present and describe the CORETRAN nominal results to the three analysis cases of Execrise2a and that were submitted as the final solution of that code. This submitted solution is here called nominal since it shows the CORETRAN results when the modeling (e.g. input data) and the analysis (e.g. boundary conditions or calculational options) are performed following strictly the benchmark specifications without any additional adjustments/tuning of the specified data. However, to follow strictly the specifications, some code modifications were necessary to implement models that are not standard in the code.

- A correction of the effective nodal density upon the bypass conditions prior to the X-S evaluation was implemented.

- The CORETRAN X-S model was not used and instead replaced by the specified interpolation routine

Moreover, although the specified transient individual channel flows were used, it would be valuable to investigate how the CORETRAN transient predictions are affected by the choice of these individual channels flows. For example, the transient total core flow could be weighted with the initial flow fraction obtained in each channel by the CORETRAN FIBWR algorithm to define the transient individual channel flows.

In addition, only the ANM-based neutronic algorithm and the 2-fluid 6-equation T/H solution scheme were used here. However, CORETRAN has been recently updated with a CMFD-based kinetic

scheme and the performance of the code using this newer algorithm should also be assessed. Similarly, the VIPRE-02 codes offers a wide-range of T/H solution schemes (e.g. drift flux) as well as constitutive closure relationships that would be valuable to investigate in order to perform a complete assessment for this PB2 exercise case.

Finally, the pressurization transient simulated here occurs very rapidly and the choice of using a constant time-step size in CORETRAN of 1ms appears here to be adequate. However, the fast nature of this transient suggests that the results are likely to be highly sensitive on the selected time-step size and a sensitivity study upon this parameter would therefore be valuable.

To summarize, although the nominal CORETRAN results presented here appear to be very satisfactory, some of the items and uncertainties discussed above need to be investigated in order to perform an in-depth assessment of the CORETRAN performance for the PB2 TT test. This will therefore be carried-out in a separate work.

6. ACKNOWLEDGEMNTS

This work was partially funded by the Swiss Federal Nuclear Safety Inspectorate (HSK[1]) and the Swiss Federal Office of energy (BFE[2]).

7. REFERENCES

[1]. L. D. Eisenhart et al. “CORETRAN-01: A Three-Dimensional Program for Reactor Core Physics and Thermal-Hydraulic Analysis – Volume 1: Theory and Numerical Analysis“, Computer Simulation and Analysis Report, WO-3574, Revision 3, November 2000, (2000)

[2] H. Ferroukhi, F. Holzgrewe, P. Coddington. “Towards a Best-Estimate Steady-State and Core Transient Analysis using the CORETRAN Code”, Proceedings ANS/ENS Intern. Meetg.on Best-estimate Methods in Nucl. Safety Installation Analysis, Washington DC, USA, November 2000, CD-ROM, paper 29, (2000)

[3] H. Ferroukhi, P. Coddington, “The Analysis of PWR and BWR Reactivity Transients with CORETRAN and RETRAN-3D”,Proceedings Tenth Intern. RETRAN Meetg, Jackson ,Wyoming, UA, October 2001, CD-ROM, paper 20, (2001)

[4] J. Solis et. al. “Boiling Water Reactor Turbine Trip (TT) Benchmark – Volume I: Final Specifications“, NEA Nuclear Science Committee, June 2001, NEA/NSC/DOC(2001)1,(2001)

[5] K. S. Smith. “An Analytical Nodal Method for Solving the Two-Group Multidimensional Static and Transient Neutron Diffusion Equations”, MIT Thesis, (1979)

[6] K.S. Smith. “Nodal Storage Reduction by Nonlinear Iteration”, *Trans.Am.Nucl.Soc*, **Volume 44**, pp.265-263, (1983)

[7] B.J. Gitnick et al. “FIBWR: A Steady-State Core Flow Distribution Code for Boiling Water Reactors, Computer Code Users Manual“, EPRI-NP-1924-CCM, (1981)

[1] Hauptabteilung für die Sicherheit der Kernanlagen
[2] Bundesamt für Energie